Glaciers in Svalbard: mass balance, runoff and freshwater flux

Jon Ove Hagen, Jack Kohler, Kjetil Melvold & Jan-Gunnar Winther

Gain or loss of the freshwater stored in Svalbard glaciers has both global implications for sea level and, on a more local scale, impacts upon the hydrology of rivers and the freshwater flux to fjords. This paper gives an overview of the potential runoff from the Svalbard glaciers. The freshwater flux from basins of different scales is quantified. In small basins ($A < 10$ km^2), the extra runoff due to the negative mass balance of the glaciers is related to the proportion of glacier cover and can at present yield more than 20% higher runoff than if the glaciers were in equilibrium with the present climate. This does not apply generally to the ice masses of Svalbard, which are mostly much closer to being in balance. The total surface runoff from Svalbard glaciers due to melting of snow and ice is roughly 25 ± 5 km^3 a^{-1}, which corresponds to a specific runoff of 680 ± 140 mm a^{-1}, only slightly more than the annual snow accumulation. Calving of icebergs from Svalbard glaciers currently contributes significantly to the freshwater flux and is estimated to be 4 ± 1 km^3 a^{-1} or about 110 mm a^{-1}.

J. O. Hagen & K. Melvold, Dept. of Physical Geography, University of Oslo, Box 1042 Blindern, NO-0316 Oslo, Norway, j.o.m.hagen@geografi.uio.no; J. Kohler & J.-G. Winther, Norwegian Polar Institute, Polar Environmental Centre, NO-9296 Tromsø, Norway.

More than half of Svalbard is covered by glaciers, and very few drainage basins are completely glacier-free. Gain or loss of the freshwater locked up in Svalbard glaciers has both global implications for sea level and more local impacts. Runoff from glaciers impacts the hydrology of rivers, and the additional discharge of freshwater from the melting glaciers also affects the stratification of the water column and, thus, the circulation within the surrounding seas and fjords. Changes in glacier discharge may significantly impact sea ice conditions around the archipelago, with consequent changes for the biota and local climate. In the most dramatic climate warming scenarios, increased freshwater contribution from this particular region could even influence deepwater production on the Svalbard shelf. In this paper information about Svalbard glaciers that may have an impact on calculations of the runoff, mainly the mass balance, will be reviewed. Some new estimates of the overall net mass balance are given, based upon which the freshwater flux derived from the glaciers is discussed.

Glaciers in Svalbard

Glaciers and ice caps cover 36 600 km^2, or about 60% of the land, of the Svalbard archipelago (Hagen et al. 1993). The eastern islands of the archipelago have the most contiguous ice coverage, linked to the coldest temperatures combined with moisture from the Barents Sea. Austfonna on Nordaustlandet in eastern Svalbard is the largest ice cap in the Eurasian Arctic at 8120 km^2 and roughly 1900 km^3 (Dowdeswell 1986; Hagen et al. 1993). Hagen et al. (1993) calculated the total ice volume of Svalbard to be approximately

7000 km^3.

Various types of glaciers are found. Most dominant by area are the large continuous ice masses divided into individual ice streams by mountain ridges and nunataks. Small cirque glaciers are also numerous, especially in the alpine mountain regions of western Spitsbergen. Several large ice caps are located in the relatively flat areas of eastern Spitsbergen, Edgeøya, Barentsøya and Nordaustlandet. These ice caps calve in the sea. The total length of the calving ice front in Svalbard is about 1000 km. All margins are grounded (Dowdeswell 1989).

Temperature conditions

The temperature conditions within the glaciers are of great importance for their flow and hydrology. Most of Svalbard's glaciers are subpolar or polythermal, which means that parts of the glacier are temperate, with temperatures at or close to the pressure melting point, and parts have temperatures below 0 °C. In the accumulation area, water percolates down into the snow and firn layers during the melting period. Due to the sub-zero temperatures in these layers, the water refreezes, releasing latent heat and raising the temperature to the melting point early in the melt season. The deep firn and ice layers remain at the pressure melting point throughout the year, resulting in a subglacial *talik* (unfrozen area) in the permafrost beneath the upper and central parts of the glaciers. Thus, water can penetrate to the bed of the glacier and feed the groundwater below the permafrost. In the ablation area, meltwater drains across the ice surface into crevasses, ice-marginal channels or moulins. No refreezing occurs within the ice, and as the annual mean surface temperatures are negative, ice temperatures remain below zero. At 15 m depth, ice temperatures are usually 2 - 3 °C above the mean annual air temperature (Hagen 1992; Björnsson et al. 1996). The thickness of the cold layer in the ablation area is usually a maximum of 80 - 100 m. Thus, for glaciers ending on land, the temperate layer does not reach the ice front, at which location there is continuous permafrost. Small glaciers (A < 10 km^2) are often not much more than 100 m thick and, therefore, the main body of these glaciers is cold. Influenced by the water temperatures at the calving front, calving glaciers have partly or completely temperate tidewater tongues.

The polythermal temperature regime of Sval-bard glaciers has been confirmed directly by measurements in boreholes drilled to bedrock and indirectly by the interpretation of ground penetrating radar (GPR) echo soundings carried out from the glacier surface (Björnsson et al. 1996; Moore et al. 1999).

The water in the temperate parts also drains during winter. In front of glaciers ending on land, the winter discharge refreezes as it flows out on frozen ground and builds up naled ice (also called "icing" or "aufeis"). Since all the glaciers in Svalbard are either cold or polythermal, the presence of naled ice indicates that the glacier is a polythermal (subpolar) glacier. At the front of tidewater glaciers, the winter runoff is released directly into the fjord.

Dynamics and surge

The flow rate of Svalbard glaciers is generally low due to the low ice temperatures and fairly low accumulation rates, usually less than 1 m a^{-1} in water equivalents (ca. 3 m of snow) even in the highest accumulation areas. In general, glaciers ending on land flow much slower than calving glaciers. Typical surface velocities are between 2 m a^{-1} in the lower ablation area and 10 m a^{-1} close to the equilibrium line altitude (ELA) for the glaciers terminating on land. At Austre Brøggerbreen (5 km^2) and Midre Lovénbreen (5 km^2), for example, only 2 m a^{-1} and 4.5 m a^{-1} have been measured close to ELA (Hagen, unpubl. data). Kronebreen, the tidewater glacier in the inner part of Kongsfjorden, is the fastest measured glacier in Svalbard. The mean annual velocity in the central part of the front of Kronebreen is 2 m d^{-1}, with a peak of 4.5 m d^{-1} at the beginning of July (Voigt 1965; Melvold 1992; Lefauconnier et al. 1994). The high velocities indicate that basal sliding is important and that the glacier sole is at the melting point. Such conditions lead to a substantial amount of water discharge and sediment transport to the fjord.

Surging glaciers are widespread in Svalbard (Liestøl 1969; Dowdeswell et al. 1991; Lefauconnier & Hagen 1991; Hagen et al. 1993; Jiskoot et al. 2000). In a non-surging glacier, there is a balance between accumulation above the ELA and the ice flux into the ablation area. Hence, the glacier maintains a near steady-state longitudinal profile. In a surge-type glacier, the ice flux is smaller than the accumulation (balance flux). Thus, the surface gradient gradually

increases, in turn causing the basal shear stress to increase. When the shear stress reaches a critical (but unknown) value, a surge can be triggered and sliding increases rapidly. The surge results in a large ice flux from the higher to the lower part of the glaciers, usually accompanied by a rapid advance of the glacier front. Often, the surge is also accompanied by a major subglacial water and sediment flux and, in the case of tidewater glaciers, by an increased iceberg production. The surge events occur independently of climatic variations, but the length of the quiescent (upbuilding) period is affected by the climate. The morphological evidence of past glacier maximum extent is therefore not necessarily directly linked to climatic conditions but rather to a surge advance (Lefauconnier & Hagen 1991).

The general retreat of calving and surging glaciers over the last hundred years has been mapped along the eastern coasts of Svalbard by Lefauconnier & Hagen (1991). The largest surge observed was at Bråsvellbreen in 1936–38 (Liestøl 1969). This outlet from the Austfonna ice cap is about 1100 km^2 and it is grounded in water in a 30 km long glacier front. During the surge the front advanced up to 20 km (Schytt 1969). Other noteworthy surges include those at Negribreen (1180 km^2) in the inner part of Storfjorden, eastern Spitsbergen, which surged in 1935–36 and advanced about 12 km in less than a year along a 15 km long section of the front, for an average speed of 35 m d^{-1} (Liestøl 1969), and the 1250 km^2 Hinlopenbreen, which surged in 1970 and calved about 2 km^3 of icebergs in a single year (Liestøl 1973).

Drainage system

The low flow velocities and the polythermal structure of the glaciers are important for the drainage system on the glaciers. Because few crevasses open, numerous meltwater channels are formed on the glacier surface during the summer. These channels gradually increase in size and melt down into the glacier. As they melt down, the ice and snow gradually close above, forming englacial channels. Since these channels follow the surface gradient of the glacier, they are usually found in a lateral position in the ablation area of the glaciers. In some places vertical moulins are formed, leading the water into the englacial and/or subglacial drainage system. The location of englacial channels has been detected using GPR; reflection hyperbola from englacial channels are readily seen in the GPR images (Hagen & Sætrang 1991; Björnsson et al. 1996).

The channel system that has gradually developed in the lower, thinner (h < 100 m), and cold parts of the glaciers is usually stable and channels reopen year after year in the same locations. This has been shown by tracer experiments (Hagen et al. 1991; Vatne 2001). The drainage pattern of the glacier is apparently stable from one year to the next; it only changes with glacier geometry changes such as when the glacier is retreating or surging. When glaciers are thicker—more than 150 - 200 m—glacier ice deformation and ice overburden pressure determine the location of water pathways. In general, the channels at the bed will follow the steepest pressure gradients, so that the main driving force for the water flow in and under glaciers is the change in the hydraulic potential.

Calculations of the hydraulic potential are based on the ice surface and ice thickness gradients. The water pressure potential at the base of a glacier can be expressed in terms of the fraction k of the local ice thickness, where k is between 0 and 1, representing the range of the water pressure in subglacial conduits from atmospheric pressure ($k=0$) to full ice overburden pressure ($k=1$). For $k=1$, the direction of the subglacial channels is decided mainly by the gradient of the ice surface (ice-directed drainage). When $k=0$, the system is open and the direction of the channels is determined by the bed gradient. When the surface and bed topography is known, the most likely location of the drainage channels at the bed can be calculated from the changes in water potential. This was done at Finsterwalderbreen in southern Spitsbergen (Hagen et al. 2000). Their modelling of the subglacial drainage indicated that the subglacial channels are partly pressurized and their location directed by the glacier except for the lowermost 1.5 km near the terminus, where the glacier is cold and thin (h < 100 m) and open, stable channels exist. Potential drainage patterns in Svalbard glaciers have also been calculated beneath Höganesbreen and Midre Lovénbreen by Melvold et al. (2002) and Rippin et al. (2003), respectively.

Glacier-dammed lakes are also readily formed on Svalbard glaciers, both in depressions on the surface and laterally. These lakes are short-lived, as they are usually emptied during the summer melt season, either by reopening of supragla-

cial or englacial channels or via subglacial channels (Liestøl et al. 1980). The supraglacial lakes are often in the size range of a few hundred to 10 000 m^3. The laterally formed lakes, usually formed in small tributary valleys of larger tidewater glaciers, can be several times as large. These lakes are often emptied by subglacial channels that usually drain directly into the fjords.

Mass balance fluctuations

Mass balance data

The annual net specific mass balance (b_n) reflects the loss or gain averaged for the glacier as a whole. The net balance is a lumped climate signal that, in Svalbard, correlates significantly with summer ablation (summer temperature) and, to a lesser degree, winter precipitation (Hagen & Liestøl 1990; Lefauconnier & Hagen 1990). Specific net balance is reported as a single number, but it can be further broken down into the summer balance

(b_s) (roughly May–September) and the winter balance (b_w) (September–May). More interesting from a climatic perspective are $b_i(z)$, the balances as a function of elevation, where i=n, w, s for net, winter, and summer, respectively. Balance as a function of elevation is a more regional quantity, as opposed to glacially averaged balance, and reflects directly the local climate at a particular elevation band.

Time series of terrestrial and aerial photographs show that most Svalbard glaciers have been retreating and thinning since around 1900 (Liestøl 1988). Since then, the retreat has been almost continuous, interrupted only by occasional surge advances. For glaciers ending on land, well preserved ice-cored moraines indicate the maximum extent. These glaciers have retreated about 1-2 km over the last hundred years. Tidewater glaciers both retreat and advance much more rapidly. The maximum extent is more difficult to locate precisely, but it can be mapped from either sub-sea moraines (Whittington et al. 1997) or historical observations. For example, the max-

imum extent of Kronebreen in 1869 was about 11 km beyond the present-day front. Over the last 50 years the front has retreated at an average rate of about 150 m a^{-1} (Liestøl 1988).

The finding that most glaciers have a negative mass balance is in accordance with this general front recession. Lefauconnier & Hagen (1990) performed a regression of meteorological records for Svalbard against observed net balance data to extrapolate the mass balance time series back to the beginning of meteorological data collection in 1912. They found that Austre Brøggerbreen has thinned by almost 40 m (more in lower parts and less in higher parts) over the period 1912–1990 and lost about 30% of its 1912 volume.

Mass balance measurements on the glaciers provide information about the total net balance, i.e. additional runoff or stored water in the catchment, but also on the total summer runoff (summer ablation) and annual accumulation (precipitation). Spot measurements of precipitation and especially snow accumulation are inaccurate because most precipitation comes as snow on strong winds, which is difficult to measure accurately with rain gauges (Førland & Hanssen-Bauer 2000). Therefore, the area distribution of the accumulation obtained by measurements on the glaciers gives much better data than weather stations. In addition, the accumulation/altitude gradient is directly observed.

Yearly mass balance components have been measured over different periods on a number of glaciers (Table 1). Those glaciers on which mass balance has been measured systematically comprise only about 0.5% of the total ice-covered area of Svalbard, but they give reliable estimates of the balance gradients and ELA in their regions and in the altitude interval they cover.

The majority of the mass balance measurements have been carried out on smaller glaciers (ca. 5 km^2) located in western and central Spitsbergen (Hagen & Liestøl 1990). The longest mass balance series are on two small glaciers, Austre Brøggerbreen (5 km^2) and Midre Lovénbreen (6 km^2), in the Kongsfjorden area of north-western Spitsbergen (Figs. 1, 2), where direct yearly measurements have been carried out continuously since 1967 and 1968 by Norwegian scientists. The glacier Kongsvegen (105 km^2), measured since 1987 (Fig. 2), extends to higher altitudes in its accumulation area than the much smaller Austre Brøggerbreen and Midre Lovénbreen (Hagen & Liestøl 1990; Lefauconnier et al. 1999). In southern Spitsbergen, Polish researchers have been measuring mass balance on Hansbreen since 1988/89 (Jania & Hagen 1996). Over shorter periods Russian scientists have studied some glaciers in western Spitsbergen (Troitskiy et al. 1975). The net balance of the measured glaciers has been generally negative during the

Table 1. Mean annual specific net mass balance (in water equivalent units) and ancillary information for the Spitsbergen glaciers at which field observations have taken place.

Glacier	Area (km^2)	Number of observations[a]	Mean net balance (m w.e. yr^{-1})	Standard deviation (mm yr^{-1})	Marine or land margin
Austre Brøggerbreen	5	36	−0.45	0.33	land
Austre Grønfjordbreen	38[c]	6	−0.63	0.20	marine[b]
Bertilbreen	5	11	−0.72	0.29	land
Bogerbreen	5	12	−0.43	0.36	land
Daudbreen	2	6	−0.36	0.27	land
Finsterwalderbreen	11	9	−0.51	0.59	land
Fridtjovbreen	49	5	−0.25	0.19	marine
Hansbreen	57	7	−0.52[d]	0.39	marine
Kongsvegen	105	16	0.00[d]	0.39	marine
Longyearbreen	4	6	−0.55	0.45	land
Midre Lovénbreen	6	35	−0.35	0.29	land
Vestre Grønfjordbreen	38[c]	4	−0.46	0.16	marine
Vøringbreen	2	18	−0.64	0.37	land

[a] The number of balance years for which measurements have been made (up to 1999).

[b] "Marine" signifies that all or part of the glacier terminus is marine.

[d] Includes losses by iceberg calving 1987–1999.

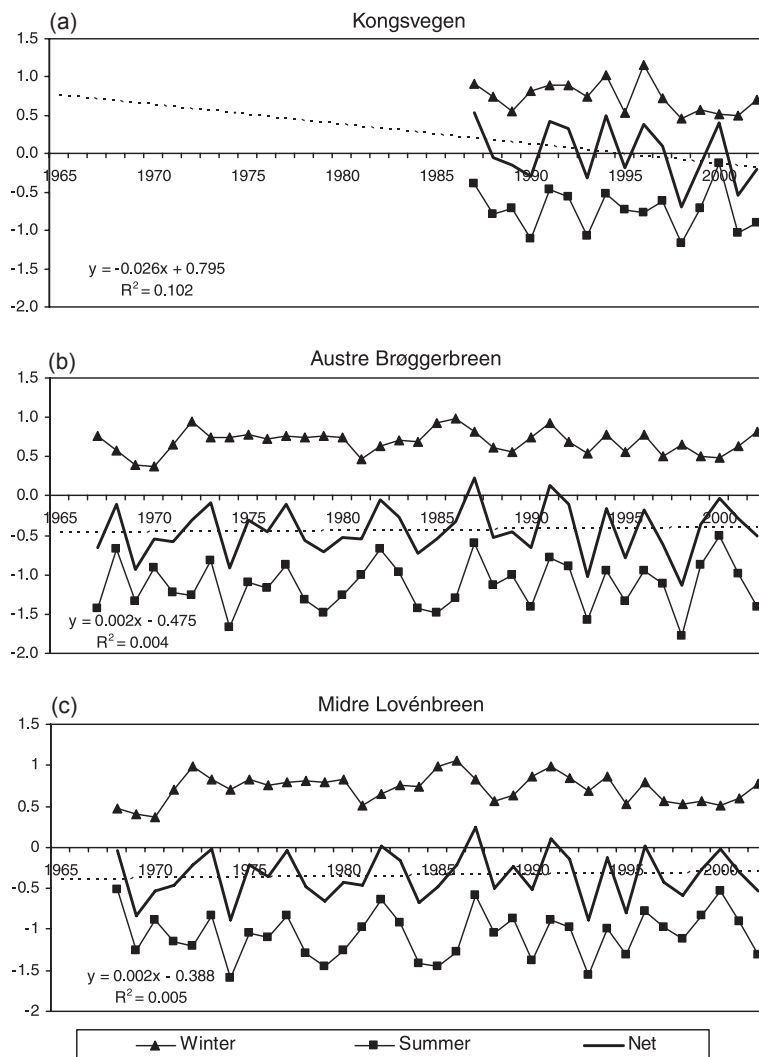[c] Area of Grønfjordbreen as a whole.

(a) Kongsvegen

$y = -0.026x + 0.795$
$R^2 = 0.102$

(b) Austre Brøggerbreen

$y = 0.002x - 0.475$
$R^2 = 0.004$

(c) Midre Lovénbreen

$y = 0.002x - 0.388$
$R^2 = 0.005$

—▲— Winter   —■— Summer   —— Net

Fig. 2. Time series of the individual mass balance components for (a) Kongsvegen (1986–2000) (105 km^2), (b) Austre Brøggerbreen (1967–2000) (5.5 km^2) and (c) Midre Lovénbreen (6 km^2), given in m water equivalents averaged over the glacier area. Note that Kongsvegen mean net balance is essentially zero. The series show no statistically significant trends.

approximately 30 years of observations (Table 1), but no statistically significant change in the trend has been observed over the last decades (Fig. 2). Most of the glaciers mentioned above are mainly below 500 m a.s.l., and have probably had a stable negative mass balance since about 1920 (Lefauconnier & Hagen 1990). The glacier area/altitude distribution is important, however; measurements on Kongsvegen indicate that glaciers covering higher accumulation areas seem to be closer to zero balance than the lower lying glaciers (Hagen 1996; Hagen et al. 2003). A recent study by Pälli et al. (in press) concludes that the low-lying glaciers Hornbreen (179 km^2 in 1980) and Hambergbreen (144 km^2 in 1980) have lost 37 - 50 %

of their volume during the last 100 years and the calving fronts have retreated by 13 - 15 km.

In addition to systematic direct mass balance measurements, there are several point measurements of mean net balance. Shallow cores have been drilled in a number of places throughout the archipelago (Fig. 1) to detect radioactive reference horizons from the fallout of 1962–63 nuclear bomb tests and from the early May 1986 Chernobyl accident (Pinglot et al. 1999; Pinglot et al. in press). The reference layers could be detected in all cores in the accumulation area of the glaciers. Cores were taken at varying altitudes from the highest part of the accumulation area downwards to below the ELA, thus providing average

net accumulation values and the net balance gradient for the ice mass accumulation areas.

Cores have also been used to obtain mass balance estimates on the larger ice caps in eastern Svalbard, where no mass balance data have been available hitherto. On the ice cap of Austfonna (8120 km^2), the largest ice cap in the archipelago (Fig. 1), an extensive study of the surface mass balance was carried out in 1998–2000, with 29 shallow ice cores and two deep ice cores retrieved. The Chernobyl layer was located in 19 of the cores, all drilled in the accumulation area, and the nuclear test layer was located in two deeper ice cores (Pinglot et al. 2001). The temporal variation of the mean annual mass balance shows that no variation occurred for different time periods, namely from 1963 to 1986 and from 1986 to 1999. The altitudinal gradient of the mean annual net mass balance and the altitude of the mean equilibrium line were obtained from five transects radiating from the crest of the ice cap showing steeper mass balance gradients than in western Svalbard (Hagen et al. 2003).

Cores can also be used together with GPR to resolve the spatial variability of snow accumulation. Pälli et al. (2002) used GPR and data from three ice cores along a radar profile on the upper parts of Nordenskjöldbreen, on Lomonosovfonna, to map spatial distribution of layering in radar images. The layers were associated with dates inferred from the cores lying on the radar profile to provide the spatial distribution of long-term accumulation. The local variability was large and GPR data were a useful tool to map the snow distribution. Winther et al. (1998) and Sand et al. (2003) measured end-of-winter snow accumulation over large areas on Svalbard, using GPR, in the years of 1997, 1998 and 1999. Measuring transects (covering both glaciated and non-glaciated areas) followed different latitudes and revealed west-to-east and south-to-north gradients of snow accumulation. On average, the east coast received over 40 % more snow than the west coast (Sand et al. 2003).

Superimposed ice and internal accumulation

The formation of internal accumulation layers and superimposed ice at the surface of High Arctic glaciers can have a significant impact on the surface mass balance and makes both direct field investigations of mass balance and remote sensing analysis complicated. Meltwater from the surface snow can percolate into the cold snowpack and refreeze, either as ice lenses in the snow and firn, or as a layer of superimposed ice on top of cold impermeable ice below. In the firn area, the meltwater may also penetrate below the previous year's summer surface and freeze as internal accumulation. Superimposed ice formation is an important source of accumulation in many Arctic glaciers and in some it is even the dominant form of accumulation (Koerner 1970; Jonsson 1982). The amount of superimposed ice varies spatially and from year to year. On Austre Brøggerbreen and Midre Lovénbreen typical values are 5 - 20 cm (Hagen & Liestøl 1990). In some areas it is even much more, but systematic measurements of superimposed ice in Svalbard glaciers are limited. The areas of superimposed ice on the Austfonna ice cap (8120 km^2) were found to cover about 30 % of the whole ice cap (Melvold, unpubl. data).

In the ablation area, the amount of superimposed ice can be measured by stakes drilled into the ice and by artificial reference horizons, but in the accumulation areas empirical modelling based on meteorological input data has often been the only way to estimate the internal accumulation from refreezing of meltwater (Woodward et al. 1997). If superimposed ice and internal accumulation are neglected in mass balance calculations, the total input of mass to the glacier may be underestimated, leading to an unrealistically negative net mass balance.

The equilibrium line altitude

The ELA can be derived from aerial photographs and satellite imagery in addition to the altitude given from the directly measured glaciers and the shallow cores. Hagen et al. (1993) published a map of the distribution of ELAs in Svalbard. However, very little information was available from the eastern part of the archipelago. The optical satellite imagery mainly gives information about the snowline, which is at higher altitudes than the actual ELA due to the formation of superimposed ice. No general function has been established between the snowline and the ELA, but the pattern of the ELA distribution is likely to have the same shape as the snowline distribution. This technique was used by Dowdeswell & Bamber (1995) to give information about the ELA pattern on the islands Barentsøya and Edgeøya in eastern Svalbard. Figure 3 shows the spatial dis-
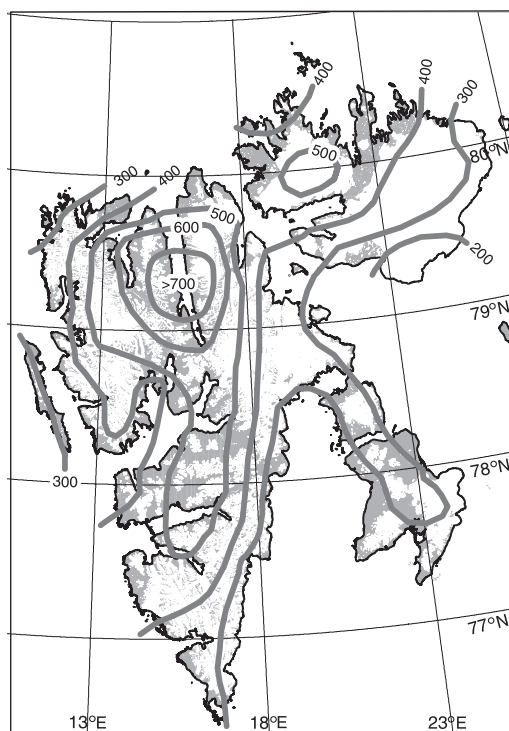
Fig. 3. Distribution pattern of the equilibrium line altitude in Svalbard (modified from Hagen et al. 2003; used with permission of *Arctic, Antarctic, and Alpine Research*.)

tribution of the present ELA (Hagen et al. 2003); the map reflects the precipitation pattern in Svalbard, with higher ELA corresponding to lower snow accumulation.

Satellite imagery can identify distinct zones on a glacier. For example, monitoring glacier mass balance with optical imagery by monitoring the ELA can be straightforward for many glaciers of the world (Hall et al. 1987; Williams et al. 1991). In Svalbard, however, the formation of superimposed ice hinders (in addition to clouds and late-summer snowfall) a precise localization of the ELA (Parrot et al. 1993; Winther 1993; Bindschadler et al. 2001). Engeset (2000), Engeset et al. (2002) and König et al. (2001) have all found that European Remote Sensing Satellite (ERS) Synthetic Aperture Radar (SAR)-derived localization of ELA on Kongsvegen does not detect the ELA, but rather detects the firn–ice transition. Even so, localization of the firn–ice transition can still provide valuable information about a glacier's climatic state. Also, König et al. (2002) were able to detect the areas of superimposed ice

formation with high precision with ERS SAR and the SAR data from the Canadian RADARSAT. Work is now underway (König, pers. comm.) to establish an operational monitoring system for the whole of Svalbard using data from European Space Agency's ERS SAR and the Advanced Synthetic Aperture Radar (ASAR) instrument on board the Environmental Satellite (ENVISAT) by means of surface type classification.

Iceberg production

The ice flux at the marine glacier margins of Svalbard, M_c, is the product of terminus velocity, ice thickness at the calving front and the horizontal width of the ice front. The average thickness of the 1000 km long calving front in the archipelago is estimated to be about 100 m (Hagen et al. 2003), although many outlet glaciers have no ground penetrating radar or marginal bathymetric data. Many of these ice fronts are relatively slow moving or stagnant, with velocities of less than 10 m a^{-1}, although some relatively fast-flowing outlet glaciers flow at 50-100 m a^{-1} (e.g. Dowdeswell & Collin 1990; Lefauconnier et al. 1994). These larger iceberg producers dominate in terms of mass.

There are few glaciers on which surface velocity measurements and calving estimates have been carried out. Lefauconnier et al. (1994) tracked ice surface features on sequential SPOT imagery to calculate ice velocity, which was combined with field measurements of terminus thickness of Kronebreen (ca. 700 km²) in Kongsfjorden in north-west Spitsbergen to yield a calving rate. With a velocity of about 2 m d^{-1}, Kronebreen is by far the fastest flowing glacier in Svalbard, as mentioned above. The annual front movement (700-800 m a^{-1}), combined with the retreat of the front, induces calving between 0.20-0.25 km³ a^{-1} (Lefauconnier et al. 1994). Due to the bathymetry beneath the glacier tongue, velocity and calving rate are expected to decrease slightly in the coming 30-50 years.

Field surveys of changing ice-cliff height, calving events and surface velocity at its marine margin have allowed the rate of mass loss to be estimated at Hansbreen (57 km²), in southern Spitsbergen (Jania & Kaczmarska 1997). A calving rate of ca. 0.02 km³ a^{-1} was found, which is an important part of the mass loss (ca. 30 %), equivalent to ca. 0.35 m a^{-1} water equivalent on the glacier surface. In Basin 5, a 670 km² drainage basin

of the ice cap Austfonna, Dowdeswell & Drewry (1989) found a velocity of ca. 40 m a^{-1} at the calving terminus. On Austfonna, flow velocities have been measured from remote sensing data by interferometry (Dowdeswell et al. 1999), but a full calculation of mass loss by calving awaits the associated marginal ice thickness data.

Over the last 50 years the glacier fronts have been generally retreating, giving larger calving rates than in a steady state situation. In Hornsund fjord (Fig. 1) the tidewater glaciers have retreated about 1 km^2 per year averaged over the last 90 years (Jania & Kaczmarska 1997).

Compiling the available information, an initial estimate of the average velocity of calving fronts through the archipelago has been calculated to be about 20-40 m a^{-1}. With an average margin thickness of 100 m and 1000 km length, the calving flux was estimated to be about 3 ± 1 km^3 a^{-1} (Hagen et al. 2003). In addition to this, the retreat of the calving glacier fronts is estimated to yield a volume of 1 km^3 a^{-1}. This estimate does not take into account the annual height change from melting. The total calving loss, M_c, is estimated to be about 4 ± 1 km^3 a^{-1}.

An additional complication to the assessment of the rate of iceberg calving within Svalbard is that a number of glaciers and ice cap drainage basins undergo periodic surges (Hagen et al. 1993; Hamilton & Dowdeswell 1996). Between the active surge advances, the termini of these ice masses are largely stagnant, contributing little mass loss through iceberg production (Melvold & Hagen 1998). In years when major Svalbard tidewater outlet glaciers surge, several cubic kilometres of ice can be released to the adjacent seas. Therefore, in years with such events the above estimate of calving rate can be far too low.

SAR investigations of ice surface velocities on Svalbard ice caps and glaciers will eventually provide, together with airborne ice penetrating radar measurements of ice thickness, a more complete data set on iceberg calving (Dowdeswell et al. 1999).

Total volume change of Svalbard glaciers

The overall net balance of Svalbard ice masses, the annual mass change (M_{tot}; change in freshwater flux) can be calculated from:

$$M_{tot} = M_a - M_m - M_c - M_b, \qquad (1)$$

where M_a is the annual surface accumulation, M_m is the mass loss by annual surface melting, M_c is loss by iceberg production and M_b is the bottom melting or freezing-on under any floating ice margins. There are no floating glacier fronts in Svalbard (Dowdeswell 1989) and M_b therefore equals zero. Total ice-mass change can then be found from the net surface mass balance $B_n = M_a - M_m$ and the iceberg calving term, M_c.

The overall net balance B_n for a region can be calculated using:

$$B_n = \sum_{i=1}^{k} b_{ni}(z) \cdot A_i \ [10^9 \ \text{m}^3], \qquad (2)$$

where $b_{ni}(z)$ are the average net balance curves as a function of the ith altitude interval and A_i is the area contained in the ith altitude interval. Areas can be derived from a 100 m horizontal resolution digital elevation model, produced from Norwegian Polar Institute 1:100 000 topographical maps (contour intervals 50 and 100 m). A Svalbard-wide mass balance curve is proposed in this paper. In Fig. 4 the long-term net balance data from several sources is combined to generate a composite balance curve, $b_{ni}(z)$. Three simple net balance curves are used to calculate the Svalbard-wide balance, two bracketing curves that define approximately the envelope of observed values, and a mean curve. Note that the long-term measured balance curves for Midre Lovénbreen, Austre Brøggerbreen and Kongsvegen encompass a fairly wide range of possible values just within one region in north-west Spitsbergen.

Combining these balance curves with the area curve, $A(z)$, for all of Svalbard (Fig. 4) in Eq. (2), an overall net balance of

$$B_n = -10 \ \text{km}^3 \pm 12 \ \text{km}^3 \ \text{a}^{-1}$$

was obtained. The overall specific surface net balance ($b_n = B_n / A$ [mm water equivalent]) comes out to be:

$$b_n = -270 \pm 330 \ \text{mm a}^{-1}.$$

The large uncertainty of ± 12 km^3 is a result of using the upper and lower mass balance curves. When adding the calving loss (M_c), estimated as -4 km$^3 \pm 1$ km^3 a^{-1}, the overall net balance of Svalbard ice massses ($M_{tot} = B_n + M_c$), is then -14.0 ± 13 km^3 a^{-1}, giving a specific total net balance of

$$m_n = -380 \pm 355 \ \text{mm a}^{-1}.$$

A weak point of the above calculation is that the net balance curves in the lower altitudes below ELA are only from one region in north-west Spitsbergen. To obtain a better spatial resolu-
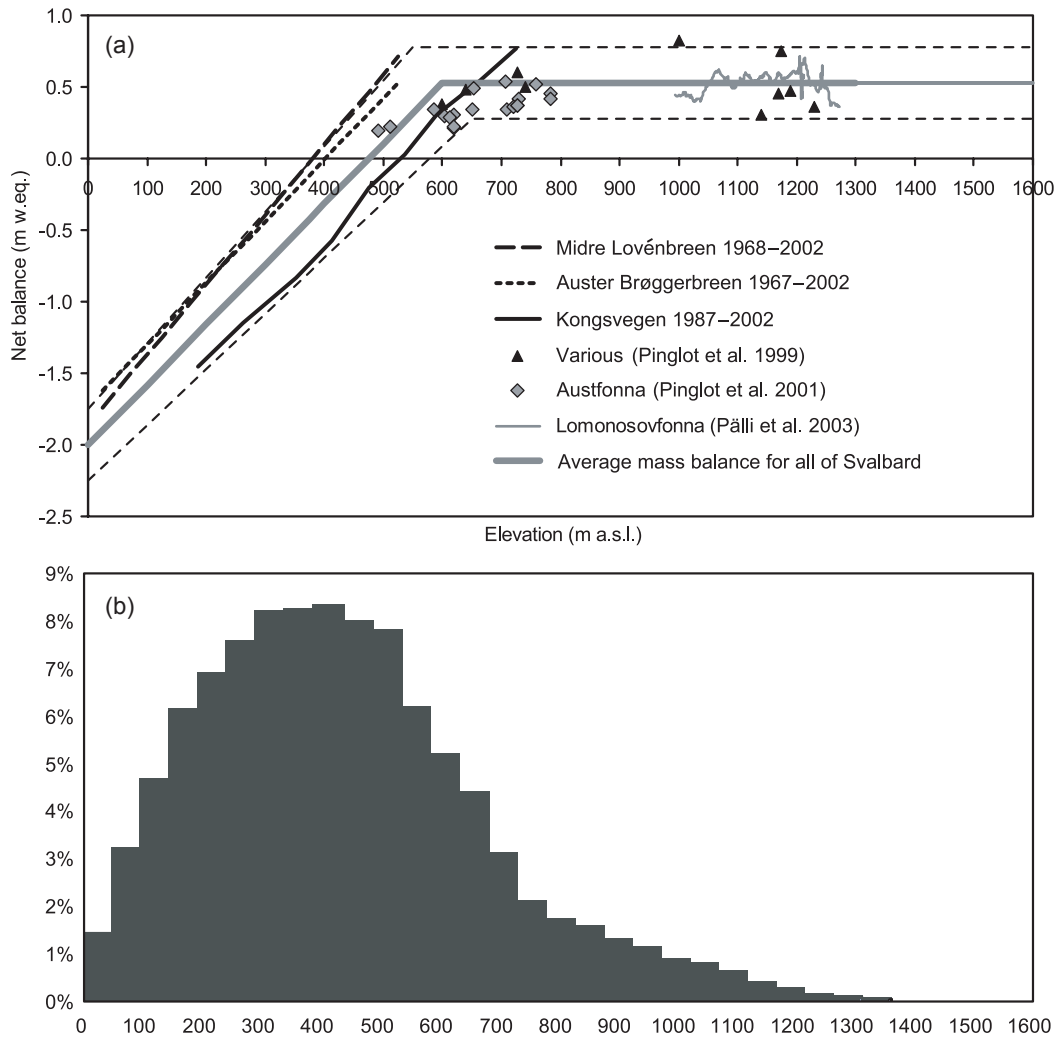
Fig. 4. (a) Average specific net balance/altitude data ($b_n[z]$) from different sources and (b) area/altitude ($A[z]$) distribution of all of the glaciers in Svalbard.

tion, Hagen et al. (2003) divided Svalbard into 13 regions and tried to establish a net balance curve ($b_{ni}[z]$) for each region, calculating the overall net balance (B_n) for each region using Eq. (2) and $A(z)$. They found that the total overall net surface balance, combining all regions, was less negative than the above mean estimate and obtained:

$$B_n = -0.5 \text{ km}^3 \pm 0.1 \text{ km}^3 \text{ a}^{-1},$$

giving the overall specific surface net balance:

$$b_n = -14 \pm 3 \text{ mm a}^{-1}.$$

When adding the calving loss as above, the over-

all net balance of Svalbard ice masses (M_{tot}), is $-4.5 \text{ km}^3 \pm 1 \text{ km}^3 \text{ a}^{-1}$, giving a specific total net balance of

$$m_n = -120 \pm 30 \text{ mm a}^{-1}.$$

The result obtained by Hagen et al. (2003) is less negative than the overall estimate in this paper even if it falls within the generous range of values defined by the bracketing mass balance curves. However, it is likely that net ablation in lower altitudes is overestimated in this overall estimate since only the balance curves from north-west Spitsbergen were used. In east-

Glaciers in Svalbard

ern Svalbard, there are only net balance data from the accumulation areas derived from core measurements. Information about the regional surface ablation below ELA is weak in both approaches, but there is less melting in the same altitude range in eastern and north-eastern Svalbard, giving a less negative overall mass balance closer to the result obtained by Hagen et al. (2003).

The contribution of Svalbard's ice caps and glaciers to global sea level change is roughly 0.01 mm a^{-1} from the Hagen et al. (2003) estimate, or 0.04 mm a^{-1} in this work, both as average values over the last 30 years. In both cases, this makes up a smaller contribution to global sea level rise than earlier estimates (0.06 mm a^{-1}), which extrapolated net mass balance data for only the smallest, most negative mass balance glaciers to the whole of Svalbard (Dowdeswell et al. 1997).

In both estimates, the net loss of mass through iceberg calving appears to be an important component of the net mass loss from Svalbard ice masses, even though the ice flow at the 1000 km long calving front is for the most part quite low and is certainly rather poorly specified.

Total accumulation and melting

The annual surface accumulation (M_a) and the annual surface melting (M_m), estimated over the Svalbard archipelago and based on the same datasets as the net balance calculations above, give a total of close to 25 ± 5 km^3 a^{-1} for the accumulation and slightly higher for the ablation. This corresponds to a specific value of 690 ± 140 mm a^{-1} of winter snow precipitation and slightly higher amount of summer runoff from surface melting. In addition, the calving flux contributes ca. 4 km$^3 \pm 1$ km^3 a^{-1}, or 110 ± 30 mm a^{-1}, giving an annual total runoff from Svalbard glaciers of ca. 800 ± 150 mm a^{-1}. In Svalbard, the freshwater flux from land through iceberg calving therefore appears to be ca. 16% of the runoff from surface melting.

Future mass balance changes

Based upon meteorological data, one simple empirical model indicates that a decrease of nearly 1 °C in the summer air temperature or an increase of 50% of the winter accumulation is required to obtain equilibrium for Austre Brøggerbreen and Midre Lovénbreen, respectively (Hagen & Liestøl 1990). The model does not take into account the effect of gradual changes in glacier area. Energy balance modelling shows similar or slightly lower values (Flemming et al. 1997). More sophisticated correlations of climate and balance can be undertaken with balance data as a function of elevation (e.g. Braithwaite 1995; Oerlemans & Reichert 2000), which would then make it possible to predict seasonal sensitivities of the glacier response to future climate scenarios. The sensitivity can then be given as change in mm water equivalents of the mass balance due to a given change in temperature or precipitation. Such calculations were done by Oerlemans et al. (unpubl. ms.), under the Response of Arctic Ice Masses to Climate Change project. The monthly and annual sensitivities were calculated for Kongsvegen and for the Austfonna ice cap. The annual mass balance sensitivity for both was an increased melting of 200-300 mm for 1 °C warming, and an increase of snow accumulation of about 100 mm for 10% increase of precipitation. The increased melting occurred in May to September.

The area/altitude distribution of the glaciers within the archipelago is important for the sensitivity of the glacier mass balance to climate changes. The present equilibrium line altitude is very close to the altitude of the bulk of the area (Fig. 4). Thus, the net surface balance, and the runoff, of Svalbard glaciers and icecaps is very sensitive to quite small changes in the ELA. A shift of a few tens of metres up or down may have a large effect on the total mass balance due to the nature of the hypsometric distribution.

Water balance in a glacierized catchment

The annual freshwater input to the fjord system can be estimated from the following water balance equation:

$$Q_{tot} = Qs + Qp + Qi + Qc + Qg + Ql - Qe, \quad (3)$$

where Q_{tot} is the potential total runoff, Qs is snowmelt from ice-free areas, Qp is runoff from rainfall in the whole basin, Qi is the glacial component of discharge which includes icemelt, firnmelt and snowmelt from the ice-covered areas, Qc is freshwater from icebergs calving from the glaciers, Qg is groundwater discharge, Ql is condensed water vapour and Qe is evaporation. The last three sources are small and combined pro-

vide an almost negligible contribution. Basal melting is negligible. Internal or basal storage is set to zero over the yearly cycle. Hagen & Lefauconnier (1995) applied this to the small basin of Bayelva, where both runoff and mass balance are measured, and showed that the glacier mass balance data can be used to provide a reliable estimate of the runoff.

The glacier mass balance measurements have provided information about the precipitation gradient (db_w/dz) and the melt rate gradient (db_s/dz) by altitude. The precipitation gradient varies, but 20-30% increase per 100 m altitude is a common value. In combination with elevation models, these gradients have been used to estimate the runoff contribution from the different sources as well as the total amount.

Mass balance data from the glaciers can be used to calculate the freshwater flux in a drainage basin and to evaluate the different sources in the water balance given in Eq. (3). This has been done for the Kongsfjorden basin in north-west Spitsbergen (Fig. 1) (Svendsen et al. 2002). The land area draining to Kongsfjorden is ca. 1430 km^2, of which 1100 km^2 is glacierized. The main summertime sources of freshwater runoff are: (1) the melting of snow and ice on the glacier surface (Qi); (2) snowmelt from areas in the drainage basin outside the glaciers (Qs); (3) rainfall (Qp) and (4) ice calving (Qc). It has been shown that in the Bayelva catchment that drains Brøggerbreen close to Ny-Ålesund (Fig. 1), the melting of snow and ice on the glaciers is the most dominant source of meltwater, giving more than two-thirds of the total runoff (Hagen & Lefauconnier 1995). They also showed that there is a very high correlation between the summer ablation and the total discharge from the glacier because the runoff variation is mainly due to warm and cold summers so ablation data (summer balance data) can be used to estimate the total runoff. The other main source for runoff variations is the summer rainfall, which can vary markedly from year to year. The snowmelt from ice-free areas gives a fairly stable contribution, as the winter snowfall does not vary much interannually (Hagen & Liestøl 1990).

Using this approach, the current mean annual total runoff to Kongsfjorden is estimated to be about 950 mm, or about 1370×10^6 m^3, or ca. 1.4 km^3 (Svendsen et al. 2002). The contributions from the different sources are shown in Table 2. The runoff due to calving is about 170 mm a^{-1},

which is about 18% of the total runoff—close to the estimated calving part of 16% for Svalbard as a whole. The total runoff of 950 mm a^{-1} is larger than the estimated 800 mm a^{-1} for the whole of Svalbard, but the Kongsfjorden basin is on the western, maritime side of Spitsbergen and is 75% glacierized compared to the average of 60% glacierization for the whole of Svalbard. Summer rainfall is not included in the runoff estimated for Svalbard overall.

At about 30%, the year-to-year runoff variations are large. The total annual runoff is not a sufficient basis for distinguishing the effects of runoff and other driving forces on the observed circulation in the fjords. This requires a quantification of the seasonal variation of runoff from the different sources. Also, more detailed information about the different sources is necessary, especially about the mass balance of the large glaciers.

The negative mass balance of some smaller glaciers and catchments may have an important impact upon the hydrology and runoff within that basin. In the basin of Bayelva (31 km^2), close to Ny-Ålesund and draining Austre and Vestre Brøggerbreen, the total mean annual runoff from the basin has been measured to 1020 mm a^{-1}, or about 30×10^6 m^3 a^{-1}. The extra runoff due to the negative mass balance of Brøggerbreen is about 200 mm a^{-1}—20% higher runoff than if the glacier were in equilibrium with the current climate (Hagen & Lefauconnier 1995).

Based on observations of temperature (degree-days) and precipitation, the runoff can also be calculated using a precipitation–runoff model. Such a model—the HBV model (Bergström 1992)—has been calibrated and applied to several catchments in Svalbard (Bruland & Sand 1994). Bru-

Table 2. Mean annual glacier runoff in Kongsfjorden from different sources calculated from mass balance data. The annual variability is shown in parentheses.

Source	Specific (mm/area)	Total (10^6 m^3)
Qi	530 (300-755)	766 (437-1096)
Qs	53 (44-62)	77 (64-90)
Qp	206 (180-50)	300 (260-360)
Qc	172 (138-207)	250 (200-300)
Qg	unknown (but small)	unknown
Ql	10	12
Qe	−20	−29
Qtotal	951 (652-1264)	1376 (944-1829)

land & Killingtveit (2002) and Bruland & Hagen (2002) applied an energy balance based on the HBV model to Austre Brøggerbreen and used, in addition to precipitation data and degree-days, energy balance data (radiation, albedo and turbulent heat flux) as well as snow-pack temperatures to calculate the runoff. The model could simulate the onset and amount of summer melt and was in good agreement with observed runoff data ($R^2 =$ ca. 0.90). The advantage of using a model like this is that daily runoff can be calculated from daily observations of meteorological data, and thus seasonal runoff events can be calculated. Bruland & Hagen (2002) showed that the model also could be used to calculate the mass balance on Austre Brøggerbreen and in sensitivity analysis of the response of future climate changes. Their calculations indicated that a mean summer temperature cooling of $1.2\,°C$ is required to obtain zero net balance, or a nearly 100 % increase of winter snow accumulation.

Conclusions and future research

Annual total runoff data can be calculated from measurements of accumulation and melting of snow and ice on the glaciers in combination with meteorological data. For the evaluation of future response to climate it will be important to monitor the mass balance components in different altitudes on the glaciers. These data will also provide both melt gradients and precipitation gradients. Mass balance measurements are only available for about 0.5 % of the glaciers in Svalbard. A more regional coverage would be useful, especially to get more information from the larger glaciers and ice caps in the eastern part of the archipelago.

In light of the warmer climate which is predicted, it will be important to get a better understanding of the effect of refreezing of meltwater in the snow and firn and the extent and amount of superimposed ice formation. It has been shown that the areas of superimposed ice formation can cover as much as 30 % of the glacier area in Svalbard. Quantifications of the refrozen volumes through modelling and direct measurements will be necessary in assessments of the sensitivity and future response of the glaciers mass balance to changes in the climate.

The future response of the glaciers can be predicted by relating glacier mass balance to meteorological data using a Seasonal Sensitivity Characteristic, outlined by Oerlemans & Reichert (2000). Using this method, the seasonal or monthly mass balance changes can be modelled by changes in temperature and precipitation based on different climate scenarios. An approach like this is currently under development under the Arctic Climate Impact Assessment programme.

The large negative mass balance as observed in many of the smaller glaciers cannot be generalized to the overall ice masses of Svalbard that have been shown to be much closer to balance. The total surface runoff from Svalbard glaciers due to melting of snow and ice was found to be close to 800 mm a^{-1}. This freshwater flux from land includes iceberg calving which appears in Svalbard to be ca. 16 % of the runoff from surface melting and is estimated to be about 4 $km^3 \pm 1$ km^3 a^{-1} or about 110 mm a^{-1}. The main calving is from point sources at outlet glaciers. In the coming years a better estimate of the calving can be obtained by airborne radar soundings of ice thickness at the glacier fronts, combined with surface velocity data obtained through interferograms of satellite images.

The impacts on the hydrology are to a great extent related to seasonal variations in the runoff. Runoff varies markedly through the melt season. In addition, the winter discharge from glaciers ending in the sea is poorly known. Daily and periodical flood events have a great impact on the sediment flux and on biota and fjord circulation. Thus, the monitoring and modelling of these events in smaller Arctic catchments will be useful.

Monitoring the altitude distribution of mass balance and the ELA will provide valuable information about the future changes in runoff. A few spot measurements combined with satellite remote sensing and modelling will be the only way to follow future changes. Satellite remote sensing techniques are capable of monitoring glacier front positions, ice velocities, surface characteristics and glacier facies. A future challenge will be to monitor glacier mass balance from space by employing remote sensing data in mass balance models. In future, there are expectations that precise laser or radar satellite altimetry such as from ICESat and CryoSat can provide direct measurements of glacier volume change. Svalbard will be used as a test site for the calibration and validation of these sensors.

References

Bindschadler, R., Dowdeswell, J., Hall, D. K. & Winther, J.-G. 2001: Glaciological applications with Landsat-7 imagery: early assessments. *Remote Sens. Environ. 78,* 163–179.

Bergström, S. 1992: *The HBV model—its structure and applications. SMHI Rep. Hydrol. 4.* Norrköping: Swedish Meteorological and Hydrological Institute.

Björnsson, H., Gjessing, Y., Hamran, S. E., Hagen, J. O., Liestøl, O., Pálsson, F. & Erlingsson, B. 1996: Temperature regime of sub-polar glaciers mapped by multi-frequency radio-echo sounding. *J. Glaciol. 42*, 23–32.

Braithwaite, R. 1995: Positive degree-day factors for ablation on the Greenland ice sheet studied by energy-balance modelling. *J. Glaciol. 41*, 153–160.

Bruland, O. & Hagen, J. O. 2002: Glacial mass balance of Austre Brøggerbreen (Spitsbergen) 1971–1999, modelled with a precipitation–runoff model. *Polar Res. 21*, 109–121.

Bruland, O. & Killingtveit, Å. 2002: An energy balance based HBV-model with application to an Arctic watershed on Svalbard, Spitsbergen. *Nord. Hydrol. 33*, 123–144.

Bruland, O. & Sand, K. 1994: The Nordic HBV-model applied to an Arctic watershed. In K. Sand & Å. Killingtveit (eds.): *Proceedings of the 10th international Northern Research Basins Symposium and Workshop, Spitsbergen, Norway. SINTEF Rep. STF22 A96415.* Pp. 594–608. Trondheim: Norwegian Institute of Technology.

Dowdeswell, J. A. 1986: Drainage-basin characteristics of Nordaustlandet ice caps, Svalbard. *J. Glaciol. 32*, 31–38.

Dowdeswell, J. A. 1989: On the nature of Svalbard icebergs. *J. Glaciol. 35*, 224–234.

Dowdeswell, J. A. & Bamber, J. L. 1995: On the glaciology of Edgeøya and Barentsøya, Svalbard. *Polar Res. 14*, 105–122.

Dowdeswell, J. A. & Collin, R. L. 1990: Fast-flowing outlet glaciers on Svalbard ice caps. *Geology 18*, 778–781.

Dowdeswell, J. A. & Drewry, D. J. 1989: The dynamics of Austfonna, Nordaustlandet, Svalbard: surface velocities, mass balance and subglacial meltwater. *Ann. Glaciol. 12*, 37–45.

Dowdeswell, J. A., Hagen, J. O., Bjørnsson, H., Glazovsky, A., Harrison, W. D., Holmlund, P., Jania, J., Koerner, R., Lefauconnier, B., Ommanney, S. & Thomas, B. 1997: The mass balance of circum-Arctic glaciers and recent climate change. *Quat. Res. 48*, 1–14.

Dowdeswell, J., Hamilton, G. & Hagen, J. O. 1991: The duration of the active phase on surge-type glaciers: contrasts between Svalbard and other regions. *J. Glaciol. 37*, 86–98.

Dowdeswell, J. A., Unwin, B., Nuttall, A.-M. & Wingham, D. J. 1999: Velocity structure, flow instability and mass flux on a large Arctic ice cap from satellite radar interferometry. *Earth Planet. Sci. Lett. 167*, 131–140.

Engeset, R. V. 2000: *Change detection and monitoring of glaciers and snow using satellite microwave imaging.* PhD thesis, University of Oslo.

Engeset, R. V., Kohler, J., Melvold, K. & Lundén, B. 2002: Change detection and monitoring of glacier mass balance and facies using ERS SAR winter images over Svalbard. *Int. J. Remote Sens. 23*, 2023–2050.

Flemming, K. M., Dowdeswell, J. A. & Orlemans, J. 1997: Modelling the mass balance of northwest Spitsbergen glaciers and response to climate change. *Ann. Glaciol. 24*, 203–210.

Førland, E. J. & Hanssen-Bauer, I. 2000: Increased precipitation in the Norwegian Arctic: true or false? *Clim. Change 46*, 485–509.

Hagen, J. O. 1992: Temperature distribution in Brøggerbreen, Lovénbreen and Kongsvegen, north west Spitsbergen. Abstract in J. O. Hagen & J. Jania (eds.): *Field workshop on glaciological research in Svalbard, current problems, Hornsund, Svalbard, May 1992.* P. 10 in part iv. Internal report. University of Silesia, Poland.

Hagen, J. O. 1996: Recent trends in mass balance of glaciers in Scandinavia and Svalbard. *Mem. Natl. Inst. Polar Res. Tokyo, Spec. Issue 51*, 343–354.

Hagen, J. O., Etzelmüller, B. & Nutall, A. M. 2000: Runoff and drainage pattern derived from Digital Elevation Models, Finsterwalderbreen, Svalbard. *Ann. Glaciol. 31*, 147–152.

Hagen, J. O., Korsen, O. M. & Vatne, G. 1991: Drainage pattern in a subpolar glacier. In Y. Gjessing et al. (eds.): *Arctic hydrology. Present and future tasks. NHK Rep. 23.* Pp. 121–131. Oslo: Norwegian National Committee for Hydrology.

Hagen, J. O. & Lefauconnier, B. 1995: Reconstructed runoff from the High Arctic basin Bayelva in Svalbard based on mass balance measurements. *Nord. Hydrol. 26*, 285–296.

Hagen, J. O. & Liestøl, O. 1990: Long term glacier mass balance investigations in Svalbard 1950–1988. *Ann. Glaciol. 14*, 102–106.

Hagen, J. O., Liestøl, O., Roland, E. & Jørgensen T. 1993: *Glacier atlas of Svalbard and Jan Mayen. Nor. Polarinst. Medd. 129.* Oslo: Norwegian Polar Institute.

Hagen, J. O., Melvold, K., Pinglot, F. & Dowdeswell, J. A. 2003: On the net mass balance of the glaciers and ice caps in Svalbard, Norwegian Arctic. *Arct. Antarct. Alp. Res. 35*, 264–270.

Hagen, J. O. & Sætrang, A. 1991: Radio-echo soundings of sub-polar glaciers with low-frequency radar. *Polar Res. 9*, 99–107.

Hall, D. K., Ormsby, J. P., Bindschadler, R. A. & Siddalingaiah, H. 1987: Characterization of snow and ice reflectance zones on glaciers using Landsat Thematic Mapper data. *Ann. Glaciol. 9*, 1–5.

Hamilton, G. S. & Dowdeswell, J. A. 1996: Controls on glacier surging in Svalbard. *J. Glaciol. 42*, 157–168.

Jania, J. & Hagen, J. O. (eds.) 1996: *Mass balance of Arctic glaciers. IASC Rep. 5.* Oslo: International Arctic Science Committee.

Jania, J. & Kaczmarska, M. 1997: Hans Glacier—a tidewater glacier in southern Spitsbergen: summary of some results. In C. J. Van der Veen (ed.): *Calving glaciers: report of a workshop, February 28–March 2, 1997. BPRC Rep. 15*, Pp. 95–104. Columbus, OH: Byrd Polar Research Center.

Jiskoot, H., Murray, T. & Boyle, P. 2000: Controls on the distribution of surge-type glaciers in Svalbard. *J. Glaciol. 46*, 412–422.

Jonsson, S. 1982: On the present glaciation of Storøya, Sval-

bard. *Geogr. Ann. 64A*, 1–2, 53–79.

Koerner, R. M. 1970: Some observations on superimposition of ice on the Devon Island Ice Cap, N.W.T., Canada. *Geogr. Ann. 52A,* 57–67.

König, M., Wadham, J., Winther, J.-G., Kohler, J. & Nuttall, A.-M. 2002: Detection of superimposed ice on the glaciers Kongsvegen and Midre Lovénbreen, Svalbard, using SAR satellite imagery. *Ann. Glaciol. 34*, 335–342.

König, M., Winther, J.-G. & Isaksson, E. 2001: Snow and glacier ice studies with satellite remote sensing—a review. *Rev. Geophys. 19*, 1–27.

Lefauconnier, B. & Hagen, J. O. 1990: Glaciers and Climate in Svalbard, statistical analysis and reconstruction of the Brøgger glacier mass balance for the last 77 years. *Ann. Glaciol. 14*, 148–152.

Lefauconnier, B. & Hagen, J. O. 1991: *Surging and calving glaciers in eastern Svalbard. Nor. Polarinst. Medd. 116.*

Lefauconnier, B., Hagen, J. O., Ørbeck, J. B., Melvold, K. & Isaksson, E. 1999: Glacier balance trends in the Kongsfjorden area, western Spitsbergen, Svalbard, in relation to the climate. *Polar Res. 18*, 307–313.

Lefauconnier, B., Hagen, J. O. & Rudant, J. P. 1994: Flow speed and calving rate of Kongsbreen Glacier, 79°N, Spitsbergen, Svalbard, using SPOT images. *Polar Res. 13*, 59–65.

Liestøl, O. 1969: Glacier surges in west Spitsbergen. *Can. J. Earth Sci. 6*, 895–987.

Liestøl, O. 1973: Glaciological work in 1971. *Nor. Polarinst. Årb. 1971,* 67–76.

Liestøl, O. 1988: The glaciers in the Kongsfjorden area, Spitsbergen. *Nor. Geogr. Tidsskr. 42*, 231–238.

Liestøl, O., Repp, K. & Wold, B. 1980: Supra-glacial lakes in Spitsbergen. *Nor. Geogr. Tidsskr. 34*, 89–92.

Melvold, K. 1992: *Studie av brebevegelse på Kongsvegen og Kronebreen, Svalbard. (Studies of glacier dynamics on Kongsvegen and Kronebreen, Svalbard.) Rapp.ser. Naturgeogr. 1.* University of Oslo.

Melvold, K. & Hagen, J. O. 1998: Evolution of a surge-type glacier in its quiescent phase: Kongsvegen, Spitsbergen, 1964–1995. *J. Glaciolo. 44*, 394–404.

Melvold, K., Vaksdal, M., Lappegard, G., Schuler, T. & Hagen, J. O. 2002: *Potensiell drenering av vann fra Svea nord gruva under Høgangesbreen. (Potential drainage of water from the coal mine Svea Nord under Høganesbreen.)* Internal report. Dept. of Physical Geography, University of Oslo.

Moore, J. C., Pälli, A., Gadek, B., Jania, J., Ludwig, F., Mochnacki, D., Glowacki, P., Blatter, H. & Isaksson, E. 1999: High resolution hydrothermal structure of Hansbreen, Spitsbergen, mapped by ground penetrating radar. *J. Glaciol. 45*, 524–532.

Oerlemans, J. & Reichert, B. K. 2000: Relating glacier mass balance to meteorological data using a Seasonal Sensitivity Characteristic (SSC). *J. Glaciol. 46*, 1–6.

Pälli, A., Kohler, J., Isaksson, E., Moore, J., Pinglot, F., Pohjola, V. & Samuelsson, H. 2002: Spatial and temporal variability of snow accumulation using ground-penetrating radar and ice cores on a Svalbard glacier. *J. Glaciol. 48*, 417–424.

Pälli, A., Moore, J., Jania, J. & Glowacki, P. in press: Glacier changes in southern Spitsbergen 1901–2000. *Ann. Glaciol. 37.*

Parrot, J. F., Lyberis, N., Lefauconnier, B. & Manby, G. 1993: SPOT multispectral data and digital terrain model for the

analysis of ice-snow fields on Arctic glaciers. *Int. J. Remote Sens. 14*, 425–440.

Pinglot, J. F., Hagen, J. O., Melvold, K., Eiken, T. & Vincent, C. 2001: A mean net accumulation pattern derived from radioactive layers and radar soundings on Austfonna ice cap, Nordaustlandet, Svalbard. *J. Glaciol. 47,* 555-566.

Pinglot, J. F., Pourchet, M., Lefauconnier, L., Hagen, J. O., Isaksson, E., Vaikmäe, R. & Kamiyama, K. 1999: Accumulation in Svalbard glaciers deduced from ice cores with nuclear tests and Chernobyl reference layers. *Polar Res. 18*, 315–321.

Pinglot, J. F., Vaikmae, R., Kamiyama, K., Igarashi, M., Fritzsche, D., Wilhelms, F., Koerner, R., Henderson, L., Isaksson, E., Winther, J-G., van de Wal, R. S. W., Fournier, M., Boisset, P. & Meijer, H. A. J. in press: Ice cores from Arctic subpolar glaciers: chronology and post depositional processes deduced from radioactivity measurements. *J. Glaciol.*

Rippin, D., Willis, I., Arnold, N., Hodson, A., Moore, J., Kohler, J. & Björnsson, H. 2003: Changes in geometry and subglacial drainage of Midre Lovénbreen, Svalbard, determined from Digital Elevation Models. *Earth Surf. Process. Landforms 28*, 273–298.

Sand, K., Winther, J.-G., Marechal, D., Bruland, O. & Melvold, K. 2003: Regional variations of snow accumulation on Spitsbergen, Svalbard in 1997–99. *Nord. Hydrol. 34*, 17–32.

Schytt, V. 1969: Some comments on glacier surges in eastern Svalbard. *Can. J. Earth Sci. 6*, 867–873.

Svendsen, H., Beszczynska-Møller, A., Hagen, J. O., Lefauconnier, B., Tverberg, V., Gerland, S., Ørbæk, J. B., Bischof, K., Papucci, C., Zajaczkowski, M., Azzolini, R., Bruland, O., Wiencke, C., Winther, J.-G., Hodson, A., Mumford, P. & Dallmann, W. 2002: The physical environment of Kongsfjorden–Krossfjorden, an Arctic fiord system in Svalbard. *Polar Res. 21*, 133–166.

Troitskiy, L. S. Zinger, E. M., Koryakin, V. S., Markin, V. A. & Mikhailov, V. I. 1975: *Oledenenye Spitsbergena (Svalbarda). (Glaciation of Spitsbergen [Svalbard].)* Moscow: Nauka.

Vatne, G. 2001: Geometry of englacial water conduits, Austre Brøggerbreen, Svalbard. *Nor. J. Geogr. 55*, 85–93.

Voigt, U. 1965: Die Bewegung der Gletscherzunge des Kongsvegen (Kingsbay, Westspitzbergen). (The movement of the glacier tongue of Kongsvegen [Kings Bay, west Spitsbergen]) *Petermanns Geogr. Mitt. 109*, 1–8.

Whittington, R. J., Forsberg, C. F. & Dowdeswell, J. A. 1997: Seismic and side-scan sonar investigations of recent sedimentation in an ice-proximal glacimarine setting, Kongsfjorden, north-west Spitsbergen. In T. A. Davies et al. (eds.): *Glaciated continental margins—an atlas of acoustic images.* Pp. 175–178. London: Chapman and Hall.

Williams Jr., R. S., Hall, D. K. & Benson, C. S. 1991: Analysis of glacier facies using satellite techniques. *J. Glaciol. 37,* 120–128.

Winther, J.-G. 1993: Landsat TM-derived and in-situ summer reflectance of glaciers in Svalbard. *Polar Res. 12*, 337–55.

Winther, J.-G., Bruland, O., Sand, K., Killingtveit, Å. & Marechal, D. 1998: Snow accumulation distribution on Spitsbergen, Svalbard, in 1997. *Polar Res. 17,* 155–164.

Woodward, J., Sharp, M. & Arendt, A. 1997: The influence of superimposed-ice formation on the sensitivity of glacier mass balance to climate change. *Ann. Glaciol. 24*, 186–190.